Principal axes for consecutive bins from bottom (bin 01) to surface (bin 12) and for depth average current were calculated. The major and minor axes, orientation and ellipticity were computed from east (u), and north (v) current components. Table 1 shows the principal axes statistics for not rotating axis (original ADCP measured data). Figs. 1 & 2 show current and variability (scatter plot and current ellipses) for different layers, as well as for depth average current. Table 2 shows principal axes for rotating axis (along-shore and cross-shore current components were calculate considering 12.3 deg anti-clockwise from east). Also Figs. 3 & 4 show current and variability among the bins and depth-averaged current for rotating data. As it is obvious from statistics and figures, after rotation the principal axes are nicely matched with EW-NS direction. But concerning the depth-average mean cross-shore current which does not vanish, we investigated the data and graphs again and realized a mistake in data handling. Unfortunately the depth-averaged mean current graph was produced based on non- rotating data. Since the cross-shore current is very sensitive to the choice of coordinate system, it showed positive values along the water column. By producing the depth-average mean current based on rotated data, the graph showed a two-layer structure i.e., offshore flow in the upper layers and onshore flow in the lower layers. Therefore Fig. 7 in the manuscript should be replaced by modified one. Fig. 5 shows the along and cross-shore currents behavior former and after rotation. We would like to thank Dr. Liu regarding his constructive comment.

Principal axes of different Bins and depth-averaged currents:

Table 1. Not rotated axis

Bin#	Major-axis (mm/s)	Minor-axis (mm/s)	Orientation (rad)	Ellipticity
1	128.51	35.01	2.887	0.728
2	142.39	34.79	2.911	0.756
3	152.51	34.58	2.924	0.773
4	160.13	34.32	2.926	0.786
5	163.71	34.93	2.925	0.787
6	166.44	36.11	2.929	0.783
7	168.37	36.14	2.934	0.785
8	168.68	37.85	2.941	0.776
9	170.13	40.89	2.942	0.76
10	171.98	46.04	2.943	0.732
11	167.12	55.58	2.929	0.667
12	167.99	66.23	2.92	0.606
Depth Average	156.93	27.51	2.927	0.825

Table 2. Rotated axis in 12.3 degrees

Bin#	Majoraxis (mm/s)	Minoraxis (mm/s)	Orientation (Rad)	Ellipticity
1	128.51	35.01	3.055	0.728
2	142.39	34.79	3.078	0.756
3	152.51	34.58	3.091	0.773
4	160.13	34.32	3.094	0.786
5	163.71	34.93	3.093	0.787
6	166.44	36.11	3.097	0.783
7	168.37	36.14	3.102	0.785
8	168.68	37.85	3.109	0.776
9	170.13	40.89	3.109	0.76
10	171.98	46.04	3.111	0.732
11	167.12	55.57	3.097	0.667
12	167.99	66.23	3.088	0.606
Depth Average	156.93	27.51	3.095	0.825

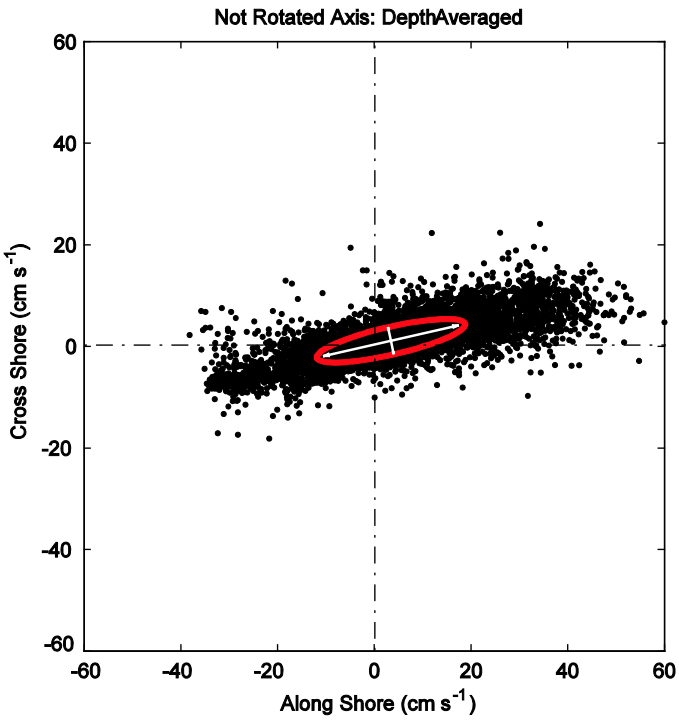

Fig. 1: Current and variability for depth-averaged not rotated data

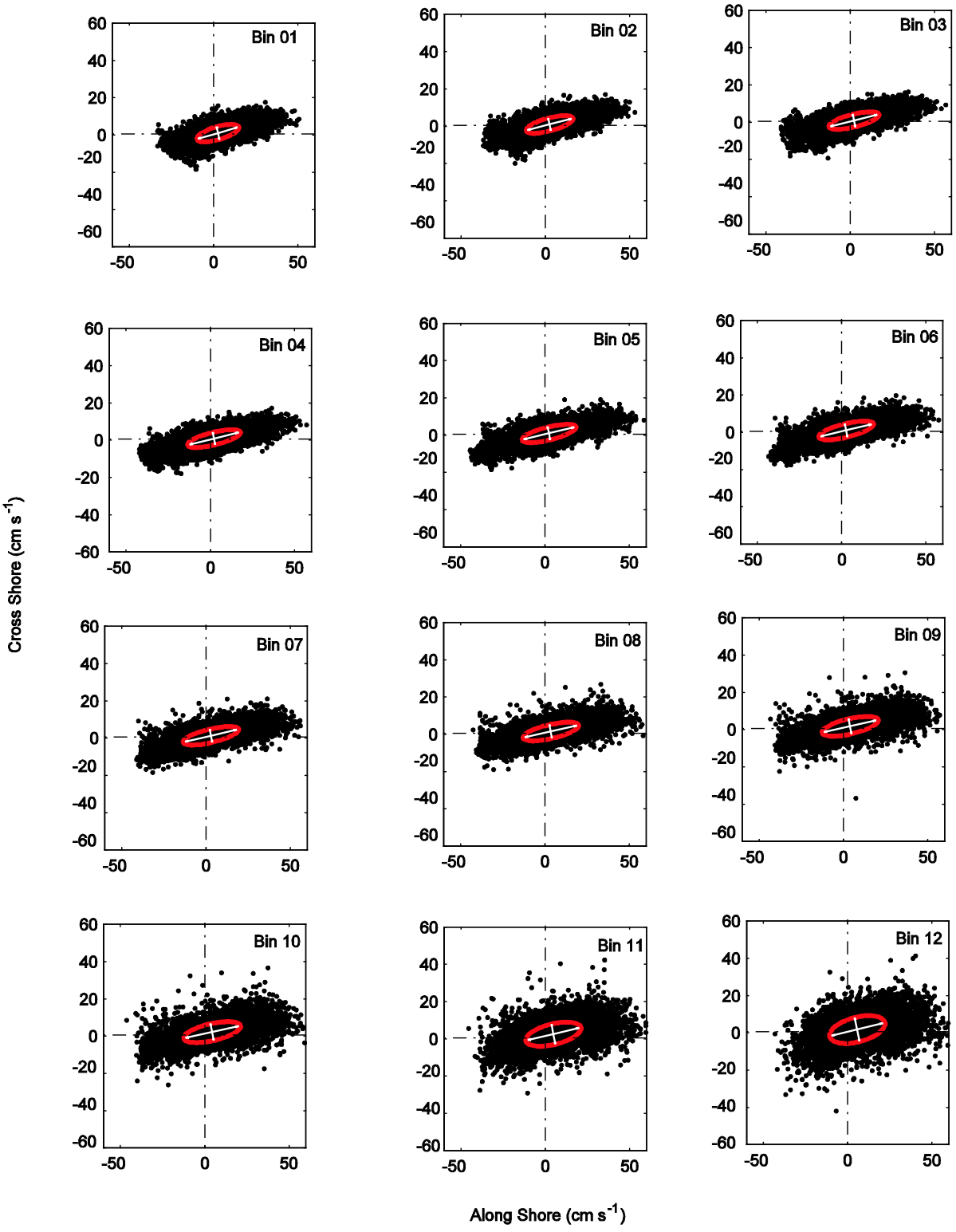

Fig. 2: Current and variability for different ADCP bins (layers) based on the not rotated data

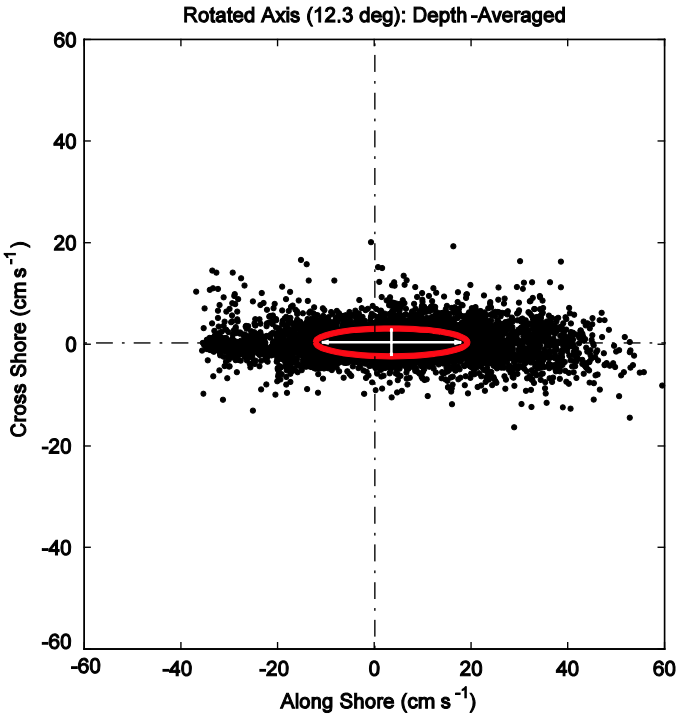

Fig. 3: Current and variability for depth-averaged current based on the rotated data (12.3 deg anti-clockwise from east)

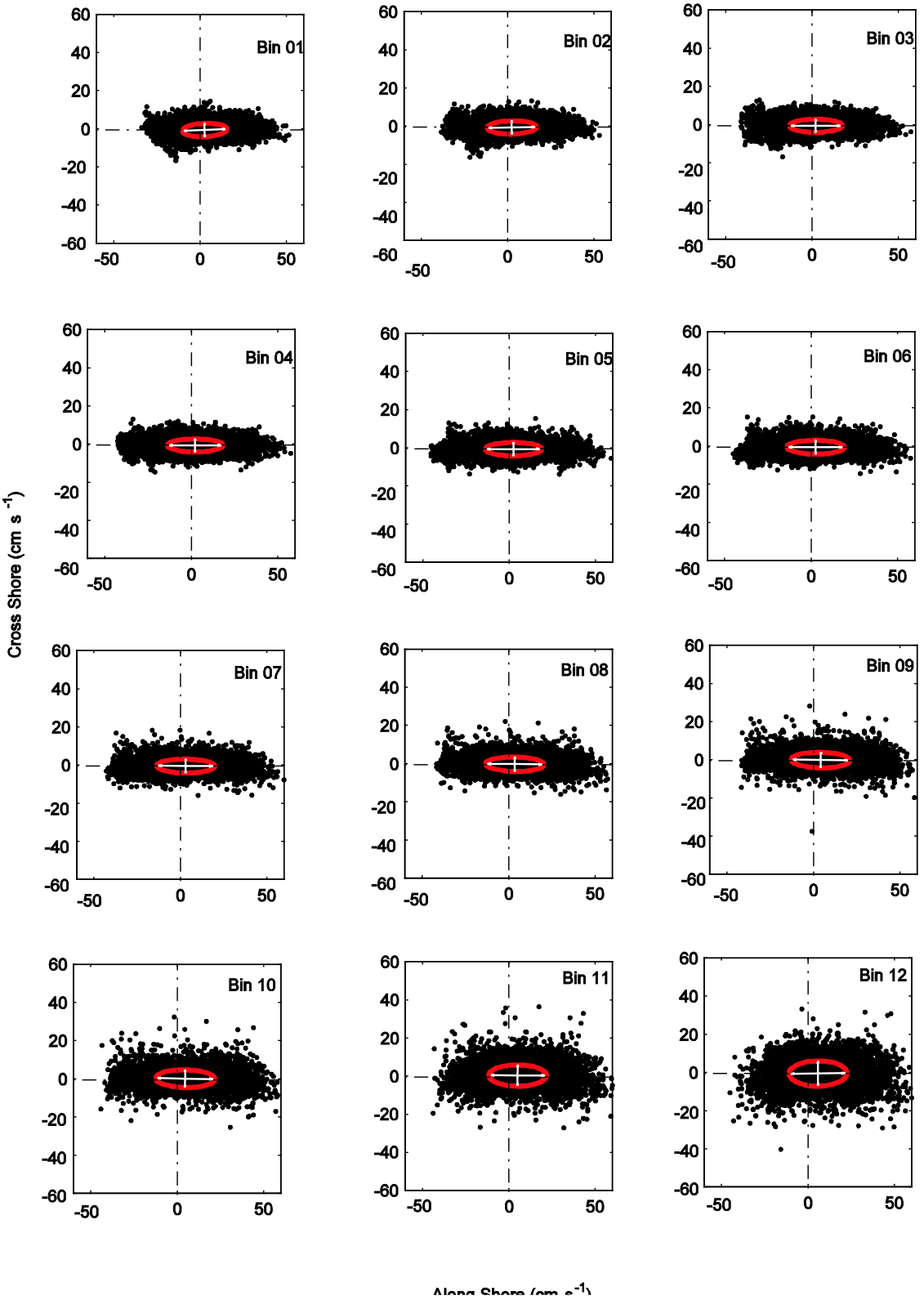

Fig. 4: Current and variability for different ADCP bins based on the rotated data (12.3 deg anti-clockwise from east)

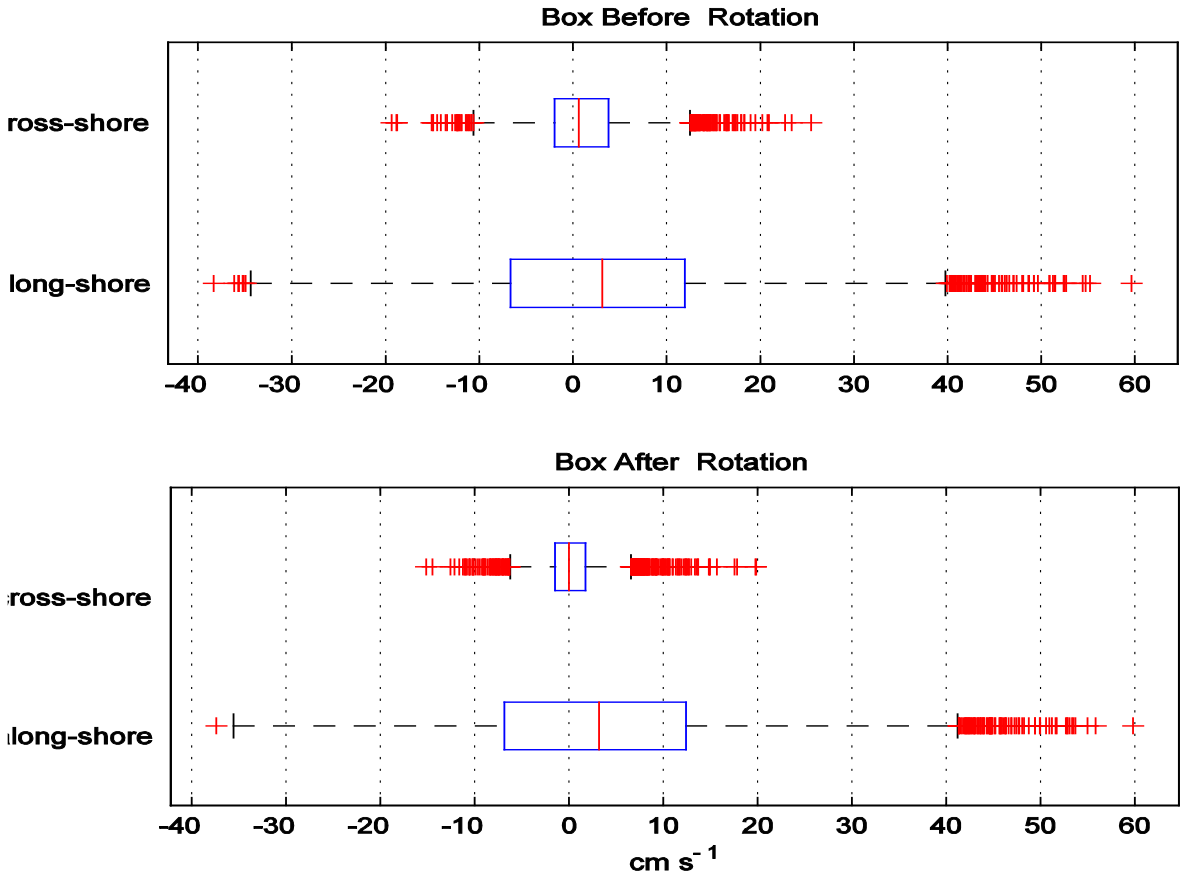

Fig. 5: Sensitivity of along-shore and cross-shore current to the coordinate system selection

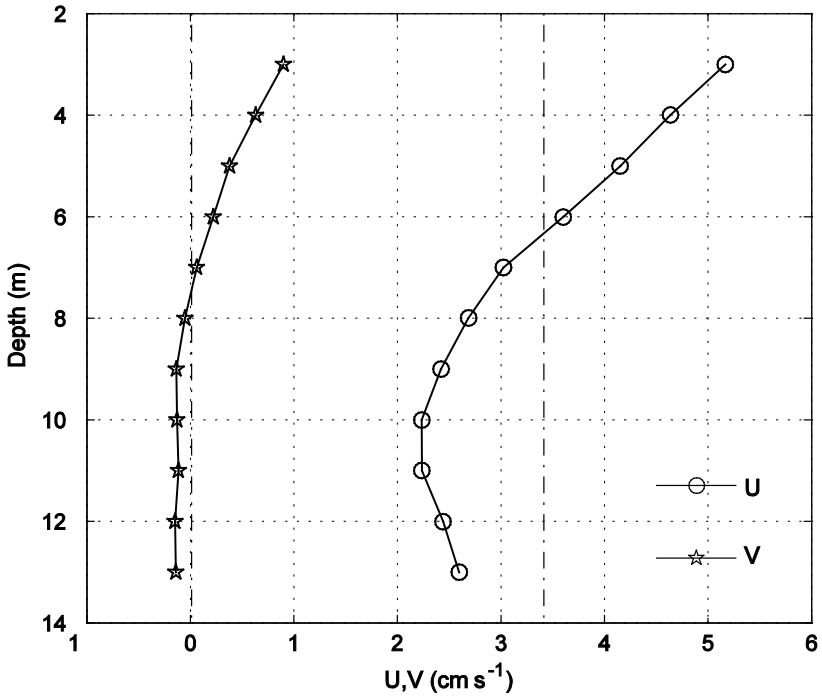

Fig. 7: Mean current components